Title

Smoking, tobacco dependence, and neurometabolites in the dorsal anterior cingulate cortex.

Journal

Molecular Psychiatry, 28(11)

Authors

ONeill, Joseph
Diaz, Maylen
Alger, Jeffry
et al.

Publication Date

2023-11-01

DOI

10.1038/s41380-023-02247-0

Peer reviewed

ARTICLE OPEN

Check for updates

Smoking, tobacco dependence, and neurometabolites in the dorsal anterior cingulate cortex

Joseph O'Neill[1,2,7], Maylen Perez Diaz[3,4,7], Jeffry R. Alger[5], Jean-Baptiste Pochon[3], Dara Ghahremani[3], Andrew C. Dean[3], Rachel F. Tyndale[6], Nicole Petersen[3], Shane Marohnic[3], Andrea Karaiskaki[3] and Edythe D. London[2,3]✉

Cigarette smoking has a major impact on global health and morbidity, and positron emission tomographic research has provided evidence for reduced inflammation in the human brain associated with cigarette smoking. Given the consequences of inflammatory dysfunction for health, the question of whether cigarette smoking affects neuroinflammation warrants further investigation. The goal of this project therefore was to validate and extend evidence of hypoinflammation related to smoking, and to examine the potential contribution of inflammation to clinical features of smoking. Using magnetic resonance spectroscopy, we measured levels of neurometabolites that are putative neuroinflammatory markers. *N*-acetyl compounds (*N*-acetylaspartate + *N*-acetylaspartylglutamate), glutamate, creatine, choline-compounds (phosphocholine + glycerophosphocholine), and *myo*-inositol, have all been linked to neuroinflammation, but they have not been examined as such with respect to smoking. We tested whether people who smoke cigarettes have brain levels of these metabolites consistent with decreased neuroinflammation, and whether clinical features of smoking are associated with levels of these metabolites. The dorsal anterior cingulate cortex was chosen as the region-of-interest because of previous evidence linking it to smoking and related states. Fifty-four adults who smoked daily maintained overnight smoking abstinence before testing and were compared with 37 nonsmoking participants. Among the smoking participants, we tested for associations of metabolite levels with tobacco dependence, smoking history, craving, and withdrawal. Levels of *N*-acetyl compounds and glutamate were higher, whereas levels of creatine and choline compounds were lower in the smoking group as compared with the nonsmoking group. In the smoking group, glutamate and creatine levels correlated negatively with tobacco dependence, and creatine correlated negatively with lifetime smoking, but none of the metabolite levels correlated with craving or withdrawal. The findings indicate a link between smoking and a hypoinflammatory state in the brain, specifically in the dorsal anterior cingulate cortex. Smoking may thereby increase vulnerability to infection and brain injury.

Molecular Psychiatry (2023) 28:4756–4765; https://doi.org/10.1038/s41380-023-02247-0

INTRODUCTION

Approximately 1.3 billion people smoke cigarettes worldwide, and there are about eight million annual smoking-related deaths [1], attributed to oncologic, respiratory, cardiovascular, and other causes [2]. The harms related to smoking likely include multiple aspects of inflammatory dysfunction. Smoking produces reactive oxygen species that promote oxidative stress and inflammation leading to carcinogenesis [3]. However, in the brain and other organs, inflammation protects against infection and aids recovery from injury [4], and there is evidence that people who smoke exhibit an attenuated inflammatory healing response [5, 6]. Positron emission tomographic (PET) studies recently added in vivo evidence of a hypoinflammatory state throughout the brains of people who smoke [7, 8]. Those studies measured the uptake of a radiotracer for the 18 kDa translocator protein (TSPO), a marker for inflammation that labels activated microglia [9]. Given the ubiquity of TSPO in the brain, especially at the blood-brain barrier [10] and its interaction with numerous ligands, such as cholesterol [11], additional studies that use alternative methods to assess potential smoking-related effects on neuroinflammation are warranted.

As detailed in several reviews [12–15], neuroinflammation may be detectable by metabolites measured with proton magnetic resonance spectroscopy (MRS). Levels of *N*-acetylaspartate + *N*-acetylaspartylglutamate (*N*-acetyl compounds, NAA) and glutamate (Glu) are diminished in wide-ranging inflammatory neurological conditions, whereas levels of creatine + phosphocreatine (Cr), choline-compounds (Cho), and *myo*-inositol (mI) are elevated. Thus, levels of these metabolites in the brain may inform questions regarding neuroinflammation in smoking and its clinical correlates.

We selected the dorsal anterior cingulate cortex (dACC) as a region-of-interest to examine this issue because functional

[1]Division of Child & Adolescent Psychiatry, Department of Psychiatry, University of California at Los Angeles, Los Angeles, CA, USA. [2]Brain Research Institute, University of California at Los Angeles, Los Angeles, CA, USA. [3]Jane and Terry Semel Institute for Neuroscience and Human Behavior and the Department of Psychiatry, University of California at Los Angeles, Los Angeles, CA, USA. [4]Biogen, Inc., Nashville, TN, USA. [5]Department of Neurology, University of California at Los Angeles, Los Angeles, CA, USA. [6]Department of Pharmacology & Toxicology, and Department of Psychiatry, University of Toronto, and Campbell Family Mental Health Research Institute, Centre for Addiction & Mental Health, Toronto, ON, Canada. [7]These authors contributed equally: Joseph O'Neill, Maylen Perez Diaz. ✉email: elondon@mednet.ucla.edu

Received: 31 March 2023 Revised: 24 August 2023 Accepted: 29 August 2023
Published online: 25 September 2023

magnetic resonance imaging (fMRI) findings have implicated the dACC in smoking-related behavioral states [16, 17]. Relevant evidence includes greater reactivity to smoking-related cues in the dACC of patients who lapsed after initiating smoking cessation compared to those who maintained abstinence [18], as well as lower activation in the dACC following behavioral therapy that diminished tobacco craving [19] and following presentation of smoking-aversive cues [20]. In addition, resting-state functional connectivity of the dACC with the insula was positively correlated with the severity of tobacco withdrawal [21].

Several prior MRS studies related to smoking have involved glutamatergic compounds in the dACC. Some of those findings were reported as Glu, others as Glx (the sum of Glu with glutamine, Gln), and still others as Glu or Glx normalized to creatine (Glu/Cr or Glx/Cr). The choice of glutamatergic endpoint has had no apparent impact on the results. Higher Glx and Glx/Cr were found in people who smoked than those who did not [22, 23], and Glx was higher during smoking satiety as compared with abstinence [22, 24]. However, one study found higher Glx and Glu and stronger functional connectivity to other cortices during tobacco withdrawal than during satiety [24]. These results are inconsistent, indicating the need for further rigorous MRS studies of the dACC, as we have attempted here. Finally, the aforementioned reduction in binding to TSPO (a marker for inflammation) among smokers was observed in the dACC among other brain regions [7, 8].

Here we compared two groups of adults with respect to MRS metabolites in the dACC—a group that smoked cigarettes and a nonsmoking control group. The hypothesis was that smoking-related hypoinflammation in the brain would manifest as elevated levels of NAA and Glu, but lower levels of Cr, Cho, and mI in participants who smoked relative to those who did not. Specifically, we posited that levels of each metabolite in the smoking group would vary from levels in nonsmoking participants in the direction opposite to that seen in known inflammatory disorders [12–15]. Although this approach risks oversimplification, we selected this straightforward strategy, reserving attempts to add complexity later if the data called for it. We additionally explored potential relationships between MRS metabolites in the dACC and clinical features of smoking—tobacco dependence, recent and lifetime exposure to smoking, cigarette craving, and psychological withdrawal.

PARTICIPANTS AND METHODS

Experimental design

After overnight (~12 h) abstinence from smoking (Time 1), adults who smoked cigarettes daily provided self-report measures of cigarette craving and withdrawal and underwent MRS for the assay of neurometabolites in the dACC. The same morning, MRS scanning was repeated 25–55 min after participants smoked their first cigarette of the day (Time 2). A nonsmoking control group was scanned at comparable times (for test-retest comparison) but without smoking. Metabolite levels were analyzed for differences between the smoking and nonsmoking groups and between Time 2 and Time 1. Within the smoking group, associations between clinical features related to smoking and metabolite levels were tested.

Participants

Participants for this study were recruited through online and print advertisements, as approved by the UCLA Institutional Review Board. During an intake session, all participants received a detailed explanation of the study procedures, gave written informed consent, and completed eligibility screening. Inclusion criteria were age 18–50 years and generally good health. Two groups were included: Individuals who smoke ("Smoking") and individuals who do not smoke ("Nonsmoking"). For the smoking group, self-report of smoking at least 5 cigarettes per day for at least 1 year was required. Smoking status was verified by a cotinine concentration ≥200 ng/ml in urine (ACCUTEST 7 Nicolet® Urine and Saliva Screen, Jant Pharmacal Corp., Encino, CA) or ≥15 ng/ml in blood [25]. Nonsmoking participants denied smoking more than 5 cigarettes at any point in their lifetime, showed negative urinary cotinine, and registered breath CO < 10 ppm at intake. Exclusions for both groups were: positive urine test for substances other than nicotine or cannabis (use of cannabis up to seven times per week was allowed), consuming more than 10 alcoholic drinks a week in the preceding month, any current psychiatric disorder other than tobacco use disorder per the Mini International Neuropsychiatric Interview for DSM-5 [26, 27], history of brain injury linked to loss of consciousness of 30 min or more, and using forms of tobacco other than cigarettes more than three times per month.

Verification of abstinence from alcohol and other drugs

Participants who met eligibility criteria returned on another day for further testing, including structural magnetic resonance imaging (MRI) and MRS scanning. Abstinence from cocaine, morphine, benzodiazepines, and amphetamines was verified with a five-panel urine drug test (Drugs of Abuse Test Insta-view®, Alfa Scientific Designs Inc., Poway, CA). Alcohol abstinence was verified using a breathalyzer (Alco-Sensor FST®, Intoximeters, Inc., St. Louis, MO). Recent abstinence from cannabis was verified with the Dräger DrugTest® 5000 saliva test (Dräger, Inc., Houston). Overnight (~12 h) abstinence from smoking was verified with the Micro + Smokerlyzer® breath CO monitor (Bedford Scientific Ltd., Maidstone, Kent, UK) with the criterion of CO in expired air <10 ppm or ≤50% the value at intake.

Self-report measures

At intake, the Fagerström Test for Nicotine Dependence (FTND) [28] was administered to assess current tobacco dependence, and the Smoking History Questionnaire (SHQ) [29] was administered to assess recent tobacco exposure (cigarettes per day over the past 30 days) and lifetime tobacco exposure (pack-years). On the scanning day, participants in the smoking group completed the Craving and Psychological Withdrawal subscales of the Shiffman–Jarvik Withdrawal Scale [30].

MR acquisition

Participants were scanned at 3 T on a Siemens Prisma with 32-channel phased-array head coil. High-resolution sagittal whole-brain T1-weighted structural MRI was acquired using a Magnetization-Prepared Rapid Gradient Echo (MPRAGE) pulse-sequence before each MRS scan that was used to position the dACC voxel and for offline MRS voxel tissue-content determination.

Water-suppressed ^{1}H MRS was acquired using single-voxel point-resolved spectroscopy (PRESS; Siemens svs_se pulse-sequence, repetition-time/echo-time = 1500/30 ms, 400 excitations, runtime 10:08 min). The acquisition voxel sampled midline (left+right) dACC, positioned approximately as in [31] (Fig. 1). The dACC voxel rested with its inferior face parallel to the dorsal corpus callosum. Left-right the voxel straddled the longitudinal fissure with its lateral faces bordering white matter. Its rostral face bordered the pregenual anterior cingulate cortex; its caudal face bordered the posterior middle cingulate cortex. Its axial-oblique dorsal face bordered the mesial superior frontal cortex. Voxel dimensions were $30 \times 30 \times 10$ mm^3 (left-right by anterior-posterior by inferior-superior) with position adjusted to maximize gray-matter content. An identical non-water-suppressed MRS voxel (8 excitations) was acquired immediately after the water-suppressed acquisition to enable water-referenced quantitation of metabolite levels. Possible head movement during MRS was checked for by comparing the brain position on rapid T1-weighted whole-brain scouts acquired before and after MRS.

MRS post-processing

Tissue composition within each MRS voxel was determined as follows: The BET and FAST tools in FSL 5.0 (www.fmrib.ox.ac.uk/fsl/) were applied to the MPRAGE volume on which each MRS voxel was positioned. This procedure yielded whole-brain gray-matter, white-matter, and cerebrospinal fluid (CSF) native-space binary masks aligned with the MPRAGE. The tissue-content in the MRS voxels was calculated using these masks. MRS voxels with over 60% CSF were rejected. Each non-water-suppressed/water-suppressed MRS voxel pair was displayed on its corresponding MPRAGE volume (Fig. 1). The MRS scan was rejected either if the voxel was not centered in the dACC or if the two voxels were not co-aligned, as confirmed by <10% disparity in tissue-composition. Similarly, voxels were compared between the two measurements for each participant and were discarded in cases of mismatch.

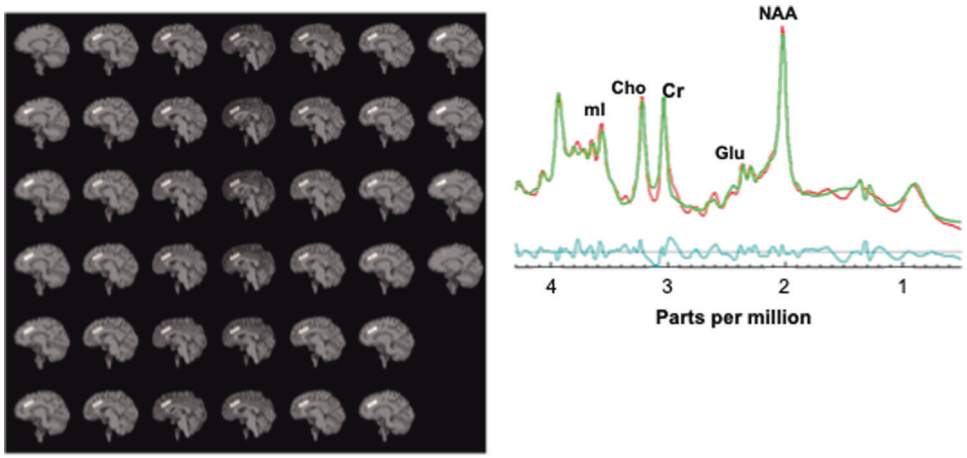

Fig. 1 Acquisition and spectral fitting of single-voxel proton magnetic resonance spectroscopy (MRS). (left) Sagittal T1w-MRI skull-stripped sections of the brain of a representative study participant showing location of MRS (PRESS TR/TE = 1500/30 ms, $30 \times 30 \times 10\,mm^3$, 400 excitations) acquisition voxel (white box) in midline dorsal anterior cingulate (dACC). (right) Sample dACC PRESS MR spectrum (plot of radiofrequency intensity *vs.* chemical shift) showing major neurometabolite resonances measured in this study. The red trace is the raw data, the green is the fit spectrum, and light blue is the residual (raw – fit) spectrum. NAA *N*-acetyl compounds, Glu glutamate, Cr creatine + phosphocreatine, Cho choline-compounds, mI myo-inositol.

MRS data from the 32 channels were combined for each water-suppressed and non-water-suppressed scan. Further processing was done with SVFit2016 [32], including time-domain filtering and non-linear least-squares spectral fitting to determine neurometabolite levels in each voxel. SVFit2016 uses the Levenberg–Marquardt implementation of the Gauss-Newton method to fit spectra in the frequency domain. The specific fitting routine is a modified version of MPFIT [33]. Fits for non-water-suppressed spectra used a model spectrum that included only a single water signal. Fits for water-suppressed spectra included models of spectra for lactate (Lac), *N*-acetylaspartate, *N*-acetylaspartylglutamate, Glu, Gln, γ-aminobutyric acid (GABA), creatine, phosphocreatine, Cho, mI, numerous low-level neurometabolites, residual water, lipids, and macromolecules. Model spectra were simulated in Versatile Simulation, Pulses, and Analysis software (VESPA) [34, 35]. Following fitting, the *N*-acetylaspartate and *N*-acetylaspartylglutamate signals were summed to total *N*-acetyl compounds ("NAA"). Similarly, creatine and phosphocreatine were summed to total creatine ("Cr"). Fit quality for all spectra was reviewed by two experts in the investigative team (JRA, JON). Non-water-suppressed spectra with excessive lipids, overly broad linewidth, distorted lineshape, or gross artifacts were rejected. Water-suppressed spectra were rejected for any of the foregoing reasons or for inadequate water-suppression or total creatine signal-to-noise ratio <5.

Metabolite levels were normalized to the unsuppressed water signal, corrected for voxel CSF-content, and expressed in Institutional Units (IU). To account for variations in gray-matter and white-matter content of the MRS voxels, metabolite levels were extrapolated to 100% gray-matter values. These "gray-matter extrapolated" values were the final endpoints for MRS data analysis.

Statistical analysis

SPSS Version 28.0 was used for statistical analyses. Mean values of demographic and drug-use variables were compared between groups using independent *T*-tests. Data were screened for outliers using the method of quartiles [36]. Individual values of MRS NAA, Glu, Glx, Cr, Cho, or mI with Cramér-Rao lower bounds (CRLB) of >20% were excluded. Linear Mixed Model (LMM) analysis, which accounts for missing values, simultaneously evaluated the main effects of group (Smoking *vs.* Nonsmoking), sex (women *vs.* men), and repeated measurement (Time 2 *vs.* Time 1), and the smoking-by-sex interaction for each MRS metabolite level in the dACC, with age as a covariate. Sex was included as an independent variable based on a priori evidence of sex differences related to smoking [37–41] and of sex differences in metabolites irrespective of smoking [42–44]. The repeated measures testing assessed the reliability of the MRS scans and, in Smoking participants, detected any effects of breaking abstinence still evident 25–55 min after smoking. Histograms and normal Q-Q plots were inspected for each metabolite level to exclude appreciable deviation from normality. For the primary Smoking *vs.* Nonsmoking group comparisons of metabolite levels, the criterion for significance was set at $p = 0.01$ (0.05/5 metabolites) two-tailed to implement Bonferroni correction for multiple comparisons. All other tests were exploratory and therefore uncorrected. The sample size was chosen using the G*Power 3.1 ANOVA: Repeated measures module to target adequate power for pre-specified effect sizes of 0.53 for smoking, 1.01 for sex, and 0.4 for repeated measurement.

Although one prior MRS study about smoking [45] calculated metabolite levels relative to water, as in this study, several others [18, 22, 24] normalized to Cr. In animal studies, nicotine exposure has been associated with altered blood brain barrier (BBB) permeability via tight junction modulation [46] and with elevated water content and aquaporin-4 (AQP4) in spinal cord [47]. Such effects could conceivably alter the value of the denominator used in water quantitation of metabolites. This possibility renders normalizing to Cr a reasonable, perhaps even preferable, alternative for smoking MRS studies. Therefore, LMM was repeated for the MRS endpoints NAA/Cr, Glu/Cr, Cho/Cr, and mI/Cr. LMM was also repeated using any demographic and drug-use variables with significant between-group differences as covariates. The variables for which this was the case were education, mother's education, and alcohol consumption (see below).

Relationships of metabolite levels with FTND score, cigarettes per day, pack-years, and the Shiffman–Jarvik subscales were also determined using Pearson correlation partialling age and sex. To test these associations, mean metabolite values of Time 1 and Time 2 were used. As noted in the Results below (except for mI/Cr), these values did not differ significantly from each other, and therefore could be collapsed.

All tests performed for Glu were repeated for Glx (see Supplemental Information). Values for GABA are not reported as some investigators do not consider GABA measured with conventional PRESS at 3 T to be reliable. Given the light level of smoking among some participants in the Smoking group (<10 cigarettes per day), all tests were repeated for a Heavier Smoking subsample ($N = 29$ participants who smoked ≥10 cigarettes per day; see Supplemental Information).

RESULTS

Demographics and clinical characteristics; tissue composition of MRS voxels

Data that passed all quality-control criteria were obtained from 54 participants in the Smoking group and 37 in the Non-smoking group (Table 1). The groups did not differ significantly in age, sex, or days of cannabis use. On average, the Smoking sample had 7% fewer years of education ($p = 0.045$), 8% fewer years of mother's education (a proxy for socioeconomic status; $p = 0.038$), and 126.5% more alcohol-drinking days ($p = 0.009$). Therefore, statistical tests were repeated including education, mother's education,

and alcohol consumption in the LMM model. A representative MR spectrum and voxel prescription are shown in Fig. 1. Group-mean CRLB values for major MRS neurometabolites are listed in Table 2. Mean voxel gray-matter, white-matter, and CSF content did not differ significantly between groups or between Time 2 and Time 1 (Table 2; all $ps > 0.05$).

Table 1. Sample characteristics and clinical measures (number or mean ± sd).

	Nonsmoking	Smoking	t/ χ^2	p
N	37	54	--	--
Age (years)	31.9 ± 7.4	33.9 ± 7.8	1.23	0.225
male/female	18/19	25/29	0.05	0.825
Education (years)	15.2 ± 2.3	14.1 ± 2.6	2.02	**0.045**
Mother's education (years)	15.2 ± 2.6	14.0 ± 2.3	2.13	**0.038**
FTND Total Score	0	4.2 ± 2.2	--	--
cigarettes/day	0	12.1 ± 5.2	--	--
pack-years	0	9.5 ± 7.2	--	--
baseline expired CO (ppm)	2.0 ± 0.9	13.0 ± 7.5	7.80	$3x10^{-14}$
Alcohol use (days/month)	3.4 ± 3.7	7.7 ± 8.7	2.70	**0.005**
Cannabis use (days/month)	3.4 ± 9.0	5.7 ± 9.8	0.68	0.504

FTND Fagerström Test of Nicotine Dependence. Statistically significant $p < 0.05$ values are in bold (independent *T*-test).

Metabolite levels: smoking status, sex, and repeated measurement (see Supplemental Information for Glx results)

Significant main effects of group for NAA, Glu, Cr, and Cho, but not for mI, were found using LMM. For the Smoking group, NAA was 11.7% higher ($F_{1,137} = 34.3$, $p < 0.001$), Glu was 31.2% higher ($F_{1,132} = 118.2$, $p < 0.001$), Cr was 5.5% lower ($F_{1,136} = 13.3$, $p < 0.001$), and Cho was 9.8% lower ($F_{1,138} = 25.1$, $p < 0.001$) than for the Nonsmoking group (Table 2, Fig. 2). These effects were significant after Bonferroni-correction for multiple comparisons. There were significant main effects of sex for Cr and Cho. Thereby, for women *vs.* men (combined Smoking and Nonsmoking samples; Fig. 2), Cr was 4.6% lower ($F_{1,136} = 5.4$, $p = 0.021$) and Cho was 11.5% lower ($F_{1,138} = 17.4$, $p < 0.001$). The group-by-sex interaction was not significant for any metabolite (all $ps > 0.05$). There was no significant main effect of sampling time on any metabolite level (Table 2; all $ps > 0.05$). Therefore, averages of Time 1 and Time 2 metabolite levels from each participant were used when computing group differences and for correlations with FTND, cigarettes per day, and pack years.

Findings for Glx were highly similar to those for Glu (Supplemental Information); findings for the Heavier Smoking subsample were highly similar to those for the entire Smoking group (Supplemental Information). All findings retained statistical significance after including education, mother's education, and alcohol consumption in LMM. Effects of alcohol consumption were ($F_{1,86} = 0.1$, $p = 0.735$) for NAA, ($F_{1,83} = 0.5$, $p = 0.470$) for Glu, ($F_{1,85} = 0.1$, $p = 0.874$) for Cr, ($F_{1,86} = 0.4$, $p = 0.508$) for Cho, and ($F_{1,86} = 1.5$, $p = 0.225$) for mI.

Table 2. LMM analysis of dACC neurometabolite levels (mean ± sd).

	Nonsmoking		Smoking	
	Time 1	Time 2	Time 1	Time 2
N	35	19	49	41
gray matter (volume %)	51.5 ± 5.9	53.8 ± 6.2	52.5 ± 4.9	52.1 ± 5.6
white matter (volume %)	35.9 ± 6.9	31.6 ± 5.2	34.5 ± 6.2	34.9 ± 7.4
CSF (volume %)	11.9 ± 4.0	13.5 ± 4.1	12.9 ± 5.4	13.0 ± 4.6
NAA (IU)	21.3 ± 2.1	20.5 ± 2.2	**23.8 ± 2.8**[a]	**23.4 ± 3.0**[a]
CRLB (%SD)	4.2 ± 0.8	4.4 ± 0.9	4.7 ± 0.7	4.6 ± 0.8
Glu (IU)	17.5 ± 1.8	17.0 ± 2.2	**22.8 ± 3.7**[a]	**22.5 ± 2.7**[a]
CRLB (%SD)	6.7 ± 2.6	6.1 ± 1.2	6.4 ± 1.8	6.4 ± 1.3
Cr (IU)	17.4 ± 1.4	16.8 ± 1.5	**16.4 ± 1.7**[a]	**16.1 ± 1.8**[a]
CRLB (%SD)	1.9 ± 0.5	2.0 ± 0.4	1.9 ± 0.4	2.0 ± 0.4
Cho (IU)	4.5 ± 0.7	4.3 ± 0.5	**4.0 ± 0.7**[a]	**3.9 ± 0.6**[a]
CRLB (%SD)	2.0 ± 0.5	2.0 ± 0.4	2.1 ± 0.5	2.1 ± 0.5
mI (IU)	11.8 ± 2.7	12.4 ± 1.7	12.6 ± 2.6	12.8 ± 2.0
CRLB (%SD)	7.3 ± 3.3	6.1 ± 2.1	6.8 ± 2.2	6.4 ± 1.8
NAA/Cr	1.22 ± 0.13	1.22 ± 0.13	**1.46 ± 0.13**[a]	**1.46 ± 0.10**[a]
Glu/Cr	1.01 ± 0.13	1.01 ± 0.15	**1.39 ± 0.20**[a]	**1.41 ± 0.14**[a]
Cho/Cr	0.26 ± 0.03	0.25 ± 0.02	**0.25 ± 0.03**[b]	**0.24 ± 0.03**[b]
mI/Cr	0.68 ± 0.14	0.74 ± 0.11	**0.77 ± 0.15**[b]	**0.80 ± 0.15**[bc]

For gray matter, white matter, or CSF there were no significant within-sample differences between Time 2 and Time 1 means or between-sample differences between Smoking and Nonsmoking means on repeated-measures linear mixed-model (LMM) accounting for sex and age. For all metabolite levels, there were no significant within-sample differences between Time 2 and Time 1 on LMM accounting for sex and age. Statistically significant values are in bold ($p < 0.01$ on LMM). [a]$p < 0.001$, [b]$p < 0.005$ main effect of Smoking *vs.* non-smoking covarying age. [c]$p < 0.05$ main effect of time.
dACC dorsal anterior cingulate cortex. *Time 1* after overnight abstinence. *Time 2* 25–55 min after the first cigarette of the morning (or corresponding times for Nonsmoking sample). *NAA N*-acetyl compounds. *Glu* glutamate. *Cr* creatine + phosphocreatine. *Cho* choline-compounds. *mI myo*-inositol. *IU* Institutional Units. *CRLB* Cramér-Rao lower bounds. *%SD* percent standard deviation.

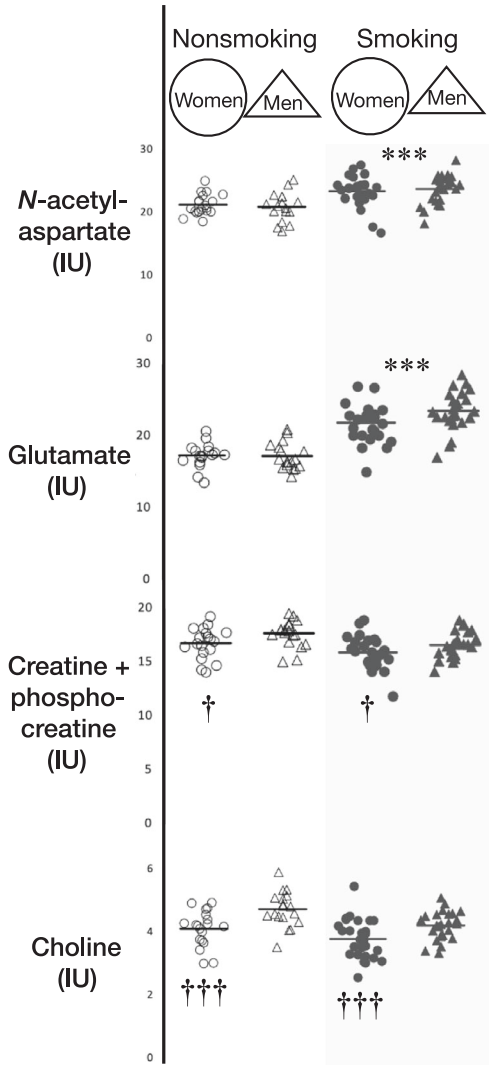

Fig. 2 Smoking *vs*. non-smoking and sex group comparisons of neurometabolite levels in the dorsal anterior cingulate cortex. *N*-acetyl compounds were 11.7% higher in the Smoking than in the Non-smoking group ($p < 0.001$). Glutamate was 31.4% higher in the Smoking (combined male and female) than in the Non-smoking group ($p < 0.001$). Creatine + phosphocreatine was 5.5% lower in the Smoking than in the Non-smoking group ($p < 0.001$). Creatine + phosphocreatine was also 4.6% lower in women than in men (combined Smoking and Nonsmoking) independent of smoking status ($p = 0.021$). Choline compounds were 9.8% lower in the Smoking than in the Nonsmoking group ($p < 0.001$) and were 11.5% lower in women than in men ($p < 0.001$). Data are averages of Time 1 and Time 2 scans. Horizontal bars represent group means. All tests are repeated-measures linear mixed model covarying age. IU Institutional Units. ***$p < 0.001$ for the Smoking vs. Nonsmoking group (combined data from women and men); †$p < 0.05$, †††$p < 0.001$ for the female vs. male group (combined Smoking and Nonsmoking).

Metabolite ratios to Cr: smoking status, sex, and repeated measurement (see Supplemental Information for Glx/Cr results)

Significant main effects of the group for NAA/Cr, Glu/Cr, Cho/Cr, and mI/Cr were found using LMM. For the Smoking group, NAA/Cr was 19.7% higher ($F_{1,135} = 154.5$, $p < 0.001$), Glu/Cr was 38.6% higher ($F_{1,132} = 189.1$, $p < 0.001$), Cho/Cr was 7.7% lower ($F_{1,136} = 8.9$, $p = 0.003$), and mI/Cr was 12.9% higher ($F_{1,136} = 9.2$, $p = 0.003$) than for the Nonsmoking group (Table 2). There were significant main effects of sex for NAA/Cr and Cho/Cr. Thereby, for women vs. men (combined Smoking and Nonsmoking groups; Fig. 2), NAA/Cr was 4.5% higher ($F_{1,135} = 8.0$, $p = 0.005$) and Cho/Cr was 8.3% lower ($F_{1,136} = 10.3$, $p = 0.002$). The group-by-sex interaction was not significant for any metabolite (all $ps > 0.05$). mI/Cr was 6.8% higher ($F_{1,136} = 4.0$, $p = 0.048$) at Time 2 than at Time 1; otherwise, there was no significant main effect of sampling time on any metabolite ratio (Table 2; all $ps > 0.05$). Thus, averages of Time 1 and Time 2 metabolite levels from each participant were used when computing group differences and for correlations with FTND, cigarettes per day, and pack years; but for mI/Cr only, separate correlations were computed for Time 1 and Time 2.

Findings for Glx/Cr were highly similar to those for Glu/Cr (Supplemental Information); findings for the Heavier Smoking subsample were highly similar to those for the entire Smoking group (Supplemental Information).

Associations of metabolite levels with smoking variables (also see Supplemental Information)

Within the Smoking sample, Glu was negatively correlated with FTND ($r = -0.34$, $p = 0.016$) and Cr was negatively correlated with FTND ($r = -0.44$, $p = 0.001$) and with pack-years ($r = -0.33$, $p = 0.017$) (Table 3, Fig. S1 Supplemental Information). No dACC metabolite was significantly associated with the Shiffman–Jarvik Craving or Psychological Withdrawal subscale scores (all $ps > 0.05$). NAA/Cr, Glu/Cr, and Cho/Cr (means of Time 1 and Time 2) were not significantly associated with any smoking variable (all ps >0.05); mI/Cr did not correlate significantly with any of these variables at Time 1 or at Time 2.

DISCUSSION

In this study of neurometabolites in the dorsal anterior cingulate cortex (dACC), NAA and Glu were higher and Cr and Cho were lower in smoking than nonsmoking research participants. Glu correlated negatively with tobacco dependence and Cr correlated negatively with both tobacco dependence and lifetime smoking history. Independent of smoking status, Cr and Cho were lower in women than men. These findings are largely consistent with a hypoinflammatory state in the dACC of people who smoke, although alternative interpretations remain viable.

Multiple putative MRS markers of neuroinflammation differed between the Smoking and Nonsmoking groups, consistent with previous evidence that people who smoke have below-control levels of inflammatory markers in the dACC [7, 8]. The present findings encompassed higher NAA and Glu and lower Cr and Cho in the Smoking group. All of these findings are consistent with the downregulation of inflammatory mediators and are in the direction opposite to that seen in many disorders that feature *increased* neuroinflammation [13] (further discussion in Supplemental Information). Similar findings were obtained for the metabolite ratios NAA/Cr, Glu/Cr, and Cho/Cr, implying that these results were not solely due to smoking-induced changes in the BBB, AQ4, or tissue water content [46, 47]. One way that smoking may induce a hypoinflammatory state in the brain is through the agonist action of nicotine (and other ligands contained in tobacco smoke) at α-7 nicotinic acetylcholine receptors (nAChRs), which are expressed in microglia [48]. By acting on α-7 nAChRs, nicotine attenuates the proinflammatory actions of microglia, including proton currents and the microglial morphological transition [49], modulating microglia towards a neuroprotective, as opposed to their better-known neuroinflammatory role [50]. The MRS findings observed here may reflect effects downstream from such actions on microglia. One should, however, note that the interaction of smoking with the immune system is complex and includes both pro-inflammatory and suppressive inflammatory effects [51, 52].

Low NAA is attested in many inflammatory conditions [13], where it is thought to reflect decreased neuronal function and viability. Additionally, in an in vitro study of human astroglial cells

Table 3. Associations of dACC MRS neurometabolite levels with tobacco dependence in Smoking group.

	FTND			CPD			Pack-Years		
	df	r	p	df	r	p	df	r	p
NAA	50	-0.26	0.059	50	-0.12	0.397	50	-0.18	0.207
Glu	**49**	**-0.34**	**0.016**	49	-0.21	0.148	49	-0.13	0.368
Cr	**49**	**-0.44**	**0.001**	49	-0.26	0.069	**49**	**-0.33**	**0.017**
Cho	50	-0.17	0.236	50	-0.07	0.602	50	-0.10	0.478
mI	50	-0.04	0.803	50	-0.10	0.485	50	-0.08	0.547

Results are for Pearson correlation partialling sex and age within the Smoking sample. Statistically significant $p < 0.05$ values are in bold.
dACC dorsal anterior cingulate cortex. *MRS* magnetic resonance spectroscopy. *FTND* Fagerström Test for Nicotine Dependence. *CPD* cigarettes per day. *NAA N*-acetyl compounds. *Glu* glutamate. *Cr* creatine + phosphocreatine. *Cho* choline-compounds. *mI myo*-inositol.

[53], NAA exerted direct anti-inflammatory actions, decreasing COX-2 protein and activating NF-κB. Elevated NAA in the Smoking group here may represent elevated neuron density or metabolic hyperactivity, and may contribute to hypoinflammation in the dACC.

Glu (or Glx or Glx/Cr) in the dACC or proximal cortices in smoking has been the focus of prior studies. Higher dACC Glu in the Smoking than the Nonsmoking group in this study is consistent with previous findings of elevated glutamatergic metabolites in dACC [22] or neighboring posterior middle cingulate [23] in people who smoke, although this finding is at variance with lower Glu in smoking participants in one report [45]. Below-control levels of Glu occur in certain inflammation-linked disorders [13] where, like low NAA, they are seen as a sign of neuronal function loss. Accordingly, we interpret *elevated* Glu in the Smoking group here as a further indication of a *hypoinflammatory* state. Evidence to support this notion includes the observation that nicotine changes the functioning and morphology of astrocytes—cells integral to Glu metabolism—without inducing their inflammatory reactive transition [54]. Further astrocytic effects of nicotine include reduction of Glu uptake through GLT1 transporters and slower conversion of Glu to Gln by astrocytic glutamine synthetase [55, 56]. Such effects increase synaptic Glu transiently, but would not likely sustain chronically elevated Glu in people who smoke. More fundamentally, such inhibitory effects would probably not lead to excess Glu as they simultaneously impede the production of astrocytic Gln that is shuttled back to the neuron where it ultimately restores Glu levels.

Although Glu was higher in the Smoking group than in the Nonsmoking group, Glu correlated negatively with nicotine dependence (FTND score) within the Smoking group. This correlation was stronger in the Heavier Smoking subsample (Supplemental Information). There are ways one might explain this counterintuitive negative correlation. It may, for example, represent a homeostatic response to keep dACC Glu levels from rising too high or, alternatively, elevated Glu may reflect a risk factor for tobacco use disorder. But, since similar correlations were not observed for Glx, Glu/Cr, or Glx/Cr, this finding should be viewed with caution.

That both NAA and Glu were higher in the Smoking group may also seem counterintuitive since Glu is neurotoxic and NAA is a marker of neuronal integrity. This apparent contradiction is resolved when one considers the distribution of Glu within brain tissue (see [57]). Most brain Glu occurs in three environments. The greatest portion of Glu is in the cytoplasm of neurons and glia; lesser fractions are found in synaptic vesicles and in glial and neuronal mitochondria [58, 59]. Due to the neurotoxicity and rapid clearance of extracellular Glu, rather little Glu exists in the synaptic cleft or other extracellular spaces in healthy brains [59]. Moreover, experiments imply that ~25% of brain Glu is "invisible" to MRS [58, 60–63], even at our TE of 30 ms [57]. Moreover, the (potentially excitotoxic) vesicular Glu is thought to belong to this invisible fraction [58, 63]. Thus, the present observed effects of smoking on Glu are unlikely to represent elevated synaptic or other extracellular Glu. Rather, they more likely reflect an adaptive shift in intracellular metabolism resulting in the expansion of the overall tissue pool of Glu, or net transfer of Glu from the invisible to the "visible" cytoplasmic environment. These mechanisms do not imply increased excitotoxicity and, hence, are quite compatible with elevated NAA.

Elevated Cr and Cho occur in inflammatory disorders [13], suggesting that low Cr and Cho in the Smoking sample here are further signs of hypoinflammation. Cr in the Smoking group additionally was lower for greater tobacco dependence and lifetime exposure. Regarding high Cho, we recently presented further evidence that it is a marker of neuroinflammation. In a placebo-controlled clinical trial, the anti-inflammatory drug ibudilast lowered Cho in white matter in patients with alcohol use disorder [64]. Cho also correlated with the volume of dilated perivascular spaces, which are associated with neuroinflammation, in white matter in Parkinson's Disease [65]. In sum, similar to prior PET evidence [7, 8], present MRS findings are consonant with dACC hypoinflammation in people who smoke.

Although hypoinflammation is a parsimonious interpretation of the present findings, alternative explanations and effects are not excluded. Various physiological roles have been posited for these metabolites, which in principle, may be influenced by smoking. NAA, for example, may reflect mitochondrial activity [66], contribute to myelin synthesis [67], and be a storage form of acetyl-CoA [68]. Glu is well known as a neurotransmitter [69] and a marker of Krebs Cycle activity [70]. Cr, in addition to its role in brain energetics buffering glycolysis and oxidative phosphorylation [71], may modulate NMDA receptors [72] and neuronal discharge [73, 74] and act as a neuroprotectant [75]. Cho is frequently cited as a marker of cell membrane turnover [71], and Cho effects could also result from energy failure, membrane degradation, angiopathy, and edema [76]. All four metabolites additionally serve as osmolytes [77]; hence their levels may have been altered by the effects of smoking on water homeostasis, although findings of the present study differed little between metabolites normed to water and metabolites normed to Cr.

Some investigators are skeptical that MRS metabolites are biomarkers of neuroinflammation at all. Counterarguments include insufficient histopathological support for neuroinflammatory interpretations of MRS findings [76]. For example, mI is often claimed to be a glial marker based on a study of juvenile rat-brain extracts whose findings may not extrapolate to humans or adults, while another study found no difference in mI between human neuronal and glioma extracts. In simian immunodeficiency virus (SIV), Cr correlated neither with the astrocyte marker glial fibrillary acidic protein (GFAP) nor with the microglial marker ionized calcium binding adaptor molecule 1 (although Cr did correlate modestly with gliosis and NAA/Cr did correlate negatively with inflammatory elements such as perivascular histiocytic infiltrates,

multinucleated giant cells, and CD14 + CD16+ monocytes in the brain). Thus, MRS markers alone are insufficient to identify neuroinflammation, and multimodal approaches are called for.

Respecting these critiques, alternative interpretations of the present MRS results are possible, but the present findings do accord with prior PET studies of smoking [7, 8]. Moreover, not all interpretations of MRS metabolites are mutually exclusive. In inflammation, activated astrocytes operate at lower energy efficiency and are diverted from their normal roles in brain energy production. Energy failure therefore could result from inflammation. Similarly, an inflammatory response can include membrane degradation and edema. The existence of alternatives does not rule-out the hypoinflammatory explanation of our findings, but the concept of MRS metabolites as markers of neuroinflammation remains in need of better support through future histopathological studies.

The level of mI was *not* lower in the Smoking group than in the Non-smoking group despite evidence that high mI is a marker of neuroinflammation [13]. A possible explanation of this negative finding is that, as stated by others [15], each neuroimaging marker of inflammation marks a different stage or aspect of inflammation, and which markers do so vary by disease. Hence, not all markers need to manifest in every condition. The only metabolite marker in the present study to show a significant elevation at Time 2 compared to Time 1 was mI/Cr; this may be further evidence of a separate role for mI relative to the other metabolites. In addition, mI may be an insensitive marker of hypoinflammation in smoking. Group differences in mI findings may have been absent in our study because mI is more difficult to quantitate at an echo-time of 30 ms, which was used here, than at shorter echo-times.

In contrast to our MRS findings, a recent study found lower NAA, Glu, Cr, and mI in participants who smoked as compared with a nonsmoking sample [45]. Although the Cr finding agrees with that observed here, the present study had no mI finding and its NAA and Glu findings were in the opposite direction. Methodological differences, particularly the prescription of the MRS voxels sampled, may have contributed to the discrepancies. Faulkner et al. sampled the right pregenual anterior cingulate cortex, which was lateral and anterior to our voxel in midline dACC. Also, their voxel contained ~50% white matter vs. 31–36% white matter in the present study. In addition, participants in the present study were on average ~10 years older, included more females, and had substantially greater lifetime smoking exposure than those studied by Faulkner et al. [45]. Our Smoking participants were tested in the morning after confirming overnight abstinence from smoking, but length of abstinence and time of scan are not reported in [45]. Finally, it is possible that Faulkner et al. obtained different mI findings because they used a shorter echo-time (8.5 ms) than in the present study.

Cr and Cho were lower in women than in men in the present study, findings that may also relate to neuroinflammation. Sex differences in neuroinflammation are widely reported [78, 79]; estradiol [80, 81] and progesterone [82, 83] have reduced neuroinflammation in preclinical studies. Given that women have higher estradiol and progesterone than men and that estrogen and progesterone help suppress neuroinflammatory responses, it is thus unsurprising that Cr and Cho were lower in women than in men.

With the exception of mI/Cr, metabolite levels and ratios did not differ significantly between Time 2 and Time 1 for either group. For the Nonsmoking group, this implies good scan-rescan reliability of the MRS measures. For the Smoking group, it does additionally suggest that the MRS findings are due to chronic, rather than acute, exposure to tobacco, as was concluded for the above-mentioned TSPO PET findings [7, 8], which were essentially the same after overnight abstinence and 15 min after smoking to satiety.

The fact that metabolite levels showed no significant associations with craving or psychological withdrawal was unexpected, given reports of higher Glx during smoking satiety than abstinence [22, 24, 84], and of higher dACC Glu accompanying greater engagement of the default mode network [18]. Additional studies matching the time-course of dACC Glu measurements with that of withdrawal and relief with smoking may clarify this issue.

There are limitations to our study. Although all participants in the Smoking group reported and provided biological evidence of daily smoking, the level of smoking in some of the samples was relatively light. Results, however, were highly similar for a Heavier Smoking subsample (Supplemental Information) as for the entire Smoking group. Our MRS voxel contained 19–52% white matter, but correction was implemented for gray-matter/white-matter content. MRS measurements were acquired in one region only, the dACC. Future studies may explore multi-voxel MRS methods for simultaneous sampling of multiple brain regions implicated in smoking-related states. In addition, sex differences observed here suggest that circulating hormones may affect the findings. Our study also included no circulatory markers of inflammation, e.g., C-reactive protein.

We report findings for Glu. MR spectra were acquired at 3 T using PRESS and 30 ms echo-time. Some investigators feel that Glu is poorly segregated from Gln under these conditions and maintain, therefore, that only Glx (Glu+Gln) should be reported (e.g., [23]). Other researchers have found it acceptable to report Glu under these conditions [85–88, and many more] and have done so in highly rigorous studies [89–91]. This decision is supported by the fact that spectral fitting programs, such as LCModel or the SVFit package used here, routinely return low CRLBs (i.e., good fits) for Glu under these conditions, especially when the data have been carefully quality controlled, as in our study. We opted to report both Glu and Glx (Supplemental Information) and found results highly similar for the two.

Strengths of the study included biological confirmation of smoking or nonsmoking status, overnight abstinence, and non-use of other drugs of abuse; rigorous quality control of all MR spectra; use of both water-referenced metabolite levels and ratios to Cr; and analysis of Glx to corroborate Glu results (see Supplemental Information). Weighing these strengths and limitations, we conclude that the present study is consistent with prior PET evidence of hypoinflammation in the dACC in tobacco use disorder. Because inflammation is a critical component of normal tissue repair and defense against infection, smoking may render the brain more susceptible to insult. A further alternative that we express with reservations but mention for balance, is that smoking may be protective against certain conditions. For example, one study showed that current smoking was associated with less severe inflammatory consequences of COVID-19 [92]. In the same study, however, the risk of severe COVID-19, hospitalization, ICU admission, and death were higher for individuals who had smoked in the past than for those who had never smoked. In addition, all-cause mortality was higher for individuals who endorsed current smoking than for those who never smoked. Smoking has also been shown to induce remission of the inflammatory condition ulcerative colitis [93].

DATA AVAILABILITY

All self-report, toxicology, and summary MRS data reported in this manuscript are publicly available from the Open Science Framework web site under project title, "Smoking, tobacco dependence, and neurometabolites in the dorsal anterior cingulate cortex" (https://osf.io/bnqsv).

REFERENCES

1. Murray CJ, Aravkin AY, Zheng P, Abbafati C, Abbas KM, Abbasi-Kangevari M et al. Global burden of 87 risk factors in 204 countries and territories, 1990–2019: a systematic analysis for the Global Burden of Disease Study 2019. Lancet. 2020; 396:1223-49.

2. US Department of Health and Human Services. The Health Consequences of Smoking–50 Years of Progress: A Report of the Surgeon General. Atlanta, GA: US Department of Health and Human Services, Centers for Disease Control and Prevention, National Center for Chronic Disease Prevention and Health Promotion, Office on Smoking and Health; 2014.
3. Caliri AW, Tommasi S, Besaratinia A. Relationships among smoking, oxidative stress, inflammation, macromolecular damage, and cancer. Mutat Res Rev Mutation Res. 2021; 787: epub ahead of print 11 January 2021; https://doi.org/10.1016/j.mrrev.2021.108365.
4. DiSabato DJ, Quan N, Godbout JP. Neuroinflammation: the devil is in the details. J Neurochem. 2016;139:136–53.
5. Reuther WJ, Brennan PA. Is nicotine still the bad guy? Summary of the effects of smoking on patients with head and neck cancer in the postoperative period and the uses of nicotine replacement therapy in these patients. Br J Oral Maxillofac Surg. 2014;52:102–105.
6. Sørensen LT. Wound healing and infection in surgery: the clinical impact of smoking and smoking cessation: a systematic review and meta-analysis. Arch Surg. 2012;147:373–83.
7. Brody AL, Gehlbach D, Garcia LY, Enoki R, Hoh C, Vera D, et al. Effect of overnight smoking abstinence on a marker for microglial activation: A [^{11}C]DAA1106 positron emission tomography study. Psychopharmacology. 2018;35:3525–34.
8. Brody AL, Hubert R, Enoki R, Garcia LY, Mamoun MS, Okita K, et al. Effect of cigarette smoking on a marker for neuroinflammation: A [^{11}C]DAA1106 positron emission tomography study. Neuropsychopharmacology. 2017;42:1630–1639.
9. Trapani A, Palazzo C, de Candia M, Lasorsa FM, Trapani G. Targeting of the translocator protein 18 kDa (TSPO): a valuable approach for nuclear and optical imaging of activated microglia. Bioconjugate Chem. 2013;24:1415–28.
10. Turkheimer FE, Edison P, Pavese N, Roncaroli F, Anderson AN, Hammers A, et al. Reference and target region modeling of [^{11}C]-(R)-PK11195 brain studies. J Nucl Med. 2007;48:158–67.
11. Kim SW, Wiers CE, Tyler R, Shokri-Kojori E, Jang YJ, Zehra A, et al. Influence of alcoholism and cholesterol on TSPO binding in brain: PET [^{11}C]PBR28 studies in humans and rodents. Neuropsychopharmacology. 2018;43:1832–1839.
12. Albrecht DS, Granziera C, Hooker JM, Loggia ML. In vivo imaging of human neuroinflammation. ACS Chem Neurosci. 2016;7:470–83.
13. Chang L, Munsaka SM, Kraft-Terry S, Ernst T. Magnetic resonance spectroscopy to assess neuroinflammation and neuropathic pain. J Neuroimmune Pharm. 2013;8:576–93.
14. Mader I, Rauer S, Gall P, Klose U. 1H MR spectroscopy of inflammation, infection and ischemia of the brain. Eur J Radio. 2008;67:250–257.
15. Quarantelli M. MRI/MRS in neuroinflammation: methodology and applications. Clin Transl Imaging. 2015;3:475–89.
16. Fedota JR, Stein EA. Resting-state functional connectivity and nicotine addiction: prospects for biomarker development. Ann NY Acad Sci. 2015;1349:64–82.
17. Hong LE, Hodgkinson CA, Yang Y, Sampath H, Ross TJ, Buchholz B, et al. A genetically modulated, intrinsic cingulate circuit supports human nicotine addiction. PNAS USA. 2010;107:13509–14.
18. Janes AC, Betts J, Jensen JE, Lukas SE. Dorsal anterior cingulate glutamate is associated with engagement of the default mode network during exposure to smoking cues. Drug Alcohol Depend. 2016;167:75–81.
19. Zhao L-Y, Tian J, Wang W, Qin W, Shi J, Li Q et al. The role of dorsal anterior cingulate cortex in the regulation of craving by reappraisal in smokers. PLoS One. 2012; 7; epub ahead of print 22 Aug 2012: https://doi.org/10.1371/journal.pone.0043598.
20. Kunas SL, Bermpohl F, Plank IS, Ströhle A, Stuke H. Aversive drug cues reduce cigarette craving and increase prefrontal cortex activation during processing of cigarette cues in quitting motivated smokers. Addiction Biol. 2022;27:e13091.
21. Ghahremani DG, Pochon J-B, Perez Diaz M, Tyndale RF, Dean AC, London ED. Functional connectivity of the anterior insula during withdrawal from cigarette smoking. Neuropsychopharmacology. 2021;46:2083–2089.
22. Mennecke A, Gossler A, Hammen T, Dörfler A, Stadlbauer A, Rösch J, et al. Physiological effects of cigarette smoking in the limbic system revealed by 3 Tesla magnetic resonance spectroscopy. J Neural Transm. 2014;121:1211–1219.
23. Schulte M, Goudriaan A, Kaag A, Kooi D, Van Den Brink W, Wiers R, et al. The effect of N-acetylcysteine on brain glutamate and gamma-aminobutyric acid concentrations and on smoking cessation: a randomized, double-blind, placebo-controlled trial. J Psychopharmacol. 2017;31:1377–1379.
24. Abulseoud OA, Ross TJ, Nam HW, Caparelli EC, Tennekoon M, Schleyer B, et al. Short-term nicotine deprivation alters dorsal anterior cingulate glutamate concentration and concomitant cingulate-cortical functional connectivity. Neuropsychopharmacology. 2020;45:1920–30.
25. Tanner J-A, Novalen M, Jatlow P, Huestis MA, Murphy SE, Kaprio J, et al. Nicotine metabolite ratio (3-hydroxycotinine/cotinine) in plasma and urine by different analytical methods and laboratories: Implications for clinical implementation measuring nicotine metabolite ratio by different methods. Cancer Epidemiol Biomark Prev. 2015;24:1239–46.
26. Hergueta T, Weiller E. Evaluating depressive symptoms in hypomanic and manic episodes using a structured diagnostic tool: validation of a new Mini International Neuropsychiatric Interview (MINI) module for the DSM-5 'With Mixed Features' specifier. Int J Bipolar Disord. 2013;1:1–10.
27. Sheehan DV, Lecrubier Y, Sheehan KH, Amorim P, Janavs J, Weiller E, et al. The mini-international neuropsychiatric interview (MINI): The development and validation of a structured diagnostic psychiatric interview for DSM-IV and ICD-10. J Clin Psychiatry. 1998;59:22–33.
28. Heatherton TF, Kozlowski LT, Frecker RC, Fagerström KO. The Fagerström Test for Nicotine Dependence: a revision of the Fagerström Tolerance Questionnaire. Br J Addict. 1991;86:1119–27.
29. Brown RA, Lejuez C, Kahler CW, Strong DR. Distress tolerance and duration of past smoking cessation attempts. J Abnorm Psychol. 2002;111:180–185.
30. Shiffman SM, Jarvik ME. Smoking withdrawal symptoms in two weeks of abstinence. Psychopharmacology. 1976;50:35–39.
31. O'Neill J, Lai TM, Sheen C, Salgari GC, Ly R, Armstrong C, et al. Cingulate and thalamic metabolites in obsessive-compulsive disorder. Psychiatry Res Neuroimaging. 2016;254:34–40.
32. Alger J, Stanovich J, Lai J, Armstrong C, Feusner J, Levitt J, et al. Performance validation of a new software package for analysis of 1H-MRS. ISMRM Workshop on MR Spectroscopy: From Current Best Practice to Latest Frontiers. Lake Constance, Germany, Aug 14-17, 2016 (Abstract). https://www.ismrm.org/workshops/Spectroscopy16/.
33. Markwardt CB. Non-linear least squares fitting in IDL with MPFIT. Proc. arXiv. 2009:0902.2850 ADASS XVIII, *ASP Conf. Ser.*, Vol. 411, eds. D. Bohlender, P. Dowler & D. Durand, 2009, p. 251 (Abstract).
34. Soher BJ, Young K, Govindaraju V, Maudsley AA. Automated spectral analysis III: application to in vivo proton MR spectroscopy and spectroscopic imaging. Magn Reson Med. 1998;40:822–31.
35. Young K, Govindaraju V, Soher BJ, Maudsley AA. Automated spectral analysis I: formation of a priori information by spectral simulation. Magn Reson Med. 1998;40:812–815.
36. Frost J. Hypothesis Testing: an intuitive guide for making data driven decisions. Statistics by Jim Publishing, State College, PA, 2020.
37. Faulkner P, Petersen N, Ghahremani DG, Cox CM, Tyndale RF, Hellemann GS, et al. Sex differences in tobacco withdrawal and responses to smoking reduced-nicotine cigarettes in young smokers. Psychopharmacology. 2018;235:193–202.
38. Garey L, Peraza N, Smit T, Mayorga NA, Neighbors C, Raines AM, et al. Sex differences in smoking constructs and abstinence: the explanatory role of smoking outcome expectancies. Psychol Addict Behav. 2018;32:660.
39. McKee SA, Smith PH, Kaufman M, Mazure CM, Weinberger AH. Sex differences in varenicline efficacy for smoking cessation: a meta-analysis. Nicotine Tob Res. 2016;18:1002–11.
40. Perez Diaz M, Pochon JB, Ghahremani DG, Dean AC, Faulkner P, Petersen N, et al. Sex differences in the association of cigarette craving with insula structure. Int J Neuropsychopharmacol. 2021;24:624–33.
41. Petersen N, London ED. Addiction and dopamine: Sex differences and insights from studies of smoking. Curr Opin Behav Sci. 2018;23:150–159.
42. Hädel S, Wirth C, Rapp M, Gallinat J, Schubert F. Effects of age and sex on the concentrations of glutamate and glutamine in the human brain. J Magn Reson Imaging. 2013;38:1480–1487.
43. Sailasuta N, Ernst T, Chang L. Regional variations and the effects of age and gender on glutamate concentrations in the human brain. Magn Reson Imaging. 2008;26:667–75.
44. Wickens MM, Bangasser DA, Briand LA. Sex differences in psychiatric disease: a focus on the glutamate system. Front Mol Neurosci. 2018;11:197.
45. Faulkner P, Lucini Paioni S, Kozhuharova P, Orlov N, Lythgoe DJ, Daniju Y, et al. Daily and intermittent smoking are associated with low prefrontal volume and low concentrations of prefrontal glutamate, creatine, myo-inositol, and N-acetylaspartate. Addict Biol. 2021; 26: epub ahead of print 3 December 2020; https://doi.org/10.1111/adb.12986.
46. Hawkins BT, Abbruscato TJ, Egleton RD, Brown RC, Huber JD, Campos CR, et al. Nicotine increases in vivo blood–brain barrier permeability and alters cerebral microvascular tight junction protein distribution. Brain Res. 2004;1027:48–58.
47. Fan ZK, Cao Y, Lv G, Wang YS, Guo ZP. The effect of cigarette smoke exposure on spinal cord injury in rats. J Neurotrauma. 2013;30:473–479.
48. Shytle RD, Mori T, Townsend K, Vendrame M, Sun N, Zeng J, et al. Cholinergic modulation of microglial activation by alpha 7 nicotinic receptors. J Neurochem. 2004;89:337–43.
49. Noda M, Kobayashi AI. Nicotine inhibits activation of microglial proton currents via interactions with α7 acetylcholine receptors. J Physiol Sci. 2017;67:235–45.
50. Suzuki T, Hide I, Matsubara A, Hama C, Harada K, Miyano K, et al. Microglial alpha7 nicotinic acetylcholine receptors drive a phospholipase C/IP3 pathway and modulate the cell activation toward a neuroprotective role. J Neurosci Res. 2006;83:1461–70.

51. Lee J, Taneja V, Vassallo R. Cigarette smoking and inflammation: Cellular and molecular mechanisms. J Dent Res. 2012;91:142–149.
52. Alrouji M, Manouchehrinia A, Gran B, Constantinescu CS. Effects of cigarette smoke on immunity, neuroinflammation and multiple sclerosis. J Neuroimmunol. 2019;329:24–34.
53. Rael LT, Thomas GW, Bar-Or R, Craun ML, Bar-Or D. An anti-inflammatory role for N-acetyl aspartate in stimulated human astroglial cells. Biochem Biophys Res Comm. 2004;319:847–53.
54. Aryal SP, Fu X, Sandin JN, Neupane KR, Lakes JE, Grady ME, et al. Nicotine induces morphological and functional changes in astrocytes via nicotinic receptor activity. Glia. 2021;69:2037–53.
55. Lim DK, Kim HS. Opposite modulation of glutamate uptake by nicotine in cultured astrocytes with/without cAMP treatment. Eur J Pharm. 2003;476:179–84.
56. Namba MD, Kupchik YM, Spencer SM, Garcia-Keller C, Goenaga JG, Powell GL et al. Accumbens neuroimmune signaling and dysregulation of astrocytic glutamate transport underlie conditioned nicotine-seeking behavior. *Addict Biol* 2020; **25**: epub ahead of print 22 July 2019; https://doi.org/10.1111/adb.12797.
57. Maddock RJ, Casazza GA, Fernandez DH, Maddock MI. Acute modulation of cortical glutamate and GABA content by physical activity. J Neurosci. 2016;36:2449–57.
58. Kauppinen RA, Pirttilä TR, Auriola SO, Williams SR. Compartmentation of cerebral glutamate in situ as detected by 1H/13C n.m.r. Biochem J. 1994;298:121–127.
59. Waagepetersen HS, Sonnewald U, Schousboe A. Glutamine, glutamate, and GABA: metabolic aspects. In: Lajtha A, Oja S, Schousboe A, Saransaari P (eds). Handbook of neurochemistry and molecular neurobiology: amino acids and peptides in the nervous system. Springer: New York, 2007, pp 1–21.
60. Bovée WM. Quantification of glutamate, glutamine, and other metabolites in in vivo proton NMR spectroscopy. NMR Biomed. 1991;4:81–84.
61. de Graaf AA, Deutz NE, Bosman DK, Chamuleau RA, de Haan JG, Bovee WM. The use of in vivo proton NMR to study the effects of hyperammonemia in the rat cerebral cortex. NMR Biomed. 1991;4:31–37.
62. Kauppinen RA, Willaims SR. Nondestructive detection of glutamate by 1H nuclear magnetic resonance spectroscopy in cortical brain slices from the guinea pig: evidence for changes in detectability during severe anoxic insults. J Neurochem. 1991;57:1136–44.
63. Pirttilä TR, Hakumäki JM, Kauppinen RA. 1H nuclear magnetic resonance spectroscopy study of cerebral glutamate in an ex vivo brain preparation of guinea pig. J Neurochem. 1993;60:1274–82.
64. Grodin EN, Nieto SJ, Meredith LR, Burnette E, O'Neill J, Alger J et al. Effects of ibudilast on central and peripheral markers of inflammation in alcohol use disorder: a randomized clinical trial. Addict Biol. 2022; 27: epub ahead of print e13182. https://doi.org/10.1111/adb.13182.
65. Donahue EK, Bui V, Foreman RP, Duran JJ, Venkadesh S, Choupan J, et al. Magnetic resonance spectroscopy shows associations between neurometabolite levels and perivascular space volume in Parkinson's disease: a pilot and feasibility study. Neuroreport. 2022;33:291–296.
66. Bates TE, Strangwald M, Keelan J, Davey GP, Munro PM, Clarke JB. Inhibition of N-acetylaspartate production: Implications for 1H MRS studies in vivo. Neuroreport. 1996;7:1397–1400.
67. Chakraborty G, Mekala P, Yahya D, Wu G, Ledeen RW. Intraneuronal N-acetylaspartate supplies acetyl groups for myelin lipid synthesis: Evidence for myelin-associated aspartoacylase. J Neurochem. 2001;78:736–45.
68. Birken DL, Oldendorf WH. N-acetyl-L-aspartic acid: A literature review of a compound prominent in 1H-NMR spectroscopic studies of brain. Neurosci Biobehav Rev. 1989;13:23–31.
69. Bennett MR, Balcar VJ. Forty years of amino acid transmission in the brain. Neurochem Int. 1999;35:269–80.
70. Sibson NR, Dhankhar A, Mason GF, Rothman DL, Behar KL, Shulman RG. Stoichiometric coupling of brain glucose metabolism and glutamatergic neuronal activity. PNAS USA. 1998;95:316–21.
71. Rae CD. A Guide to the metabolic pathways and function of metabolites observed in human brain 1H magnetic resonance spectra. Neurochem Res. 2014;39:1–36.
72. Oliveira MS, Furian AF, Fighera MR, Fiorenza NG, Ferreira J, Rubin MA, et al. The involvement of the polyamines binding sites at the NMDA receptor in creatine-induced spatial learning enhancement. Behav Brain Res. 2008;187:200–204.
73. Royes LF, Fighera MR, Furian AF, Oliveira MS, Fiorenza NG, Ferreira J, et al. Neuromodulatory effect of creatine on extracellular action potentials in rat hippocampus: role of NMDA receptors. Neurochem Int. 2008;53:33–37.
74. Andres RH, Ducraya AD, Schlattner U, Wallimann T, Widmer HR. Functions and effects of creatine in the central nervous system. Brain Res Bull. 2008;76:329–43.
75. Genius J, Geiger J, Bender A, Moller H-J, Klopstock T, Rujescu D. Creatine protects against excitotoxicity in an in vitro model of neurodegeneration. PLoS ONE. 2012; 7: epub ahead of print 8 February 2012; https://doi.org/10.1371/journal.pone.0030554.
76. Zahr NM, Mayer D, Rohlfing T, Sullivan EV, Pfefferbaum A. Imaging neuroinflammation? A perspective from MR spectroscopy. Brain Pathol. 2014;24:654–64.
77. Ross B, Bluml S. Magnetic resonance spectroscopy of the human brain. Anat Rec. 2001;265:54–84.
78. Acosta-Martínez M. Shaping microglial phenotypes through estrogen receptors: relevance to sex-specific neuroinflammatory responses to brain injury and disease. J Pharm Exp Ther. 2020;375:223–36.
79. Azcoitia I, Barreto GE, Garcia-Segura LM. Molecular mechanisms and cellular events involved in the neuroprotective actions of estradiol. Analysis of sex differences. Front Neuroendocrinol. 2019; 55:epub ahead of print 9 September 2019; https://doi.org/10.1016/j.yfrne.2019.100787. Epub 2019 Sep 9.
80. Giraud SN, Caron CM, Pham-Dinh D, Kitabgi P, Nicot AB. Estradiol inhibits ongoing autoimmune neuroinflammation and NFkappaB-dependent CCL2 expression in reactive astrocytes. PNAS USA. 2010;107:8416–21.
81. Spence RD, Wisdom AJ, Cao Y, Hill HM, Mongerson CR, Stapornkul B, et al. Estrogen mediates neuroprotection and anti-inflammatory effects during EAE through ERα signaling on astrocytes but not through ERβ signaling on astrocytes or neurons. J Neurosci. 2013;33:10924–33.
82. De Nicola AF, Garay LI, Meyer M, Guennoun R, Sitruk-Ware R, Schumacher M et al. Neurosteroidogenesis and progesterone anti-inflammatory/neuroprotective effects. J Neuroendocrinol. 2018; 30: epub ahead of print e12502. https://doi.org/10.1111/jne.12502.
83. Pettus EH, Wright DW, Stein DG, Hoffman SW. Progesterone treatment inhibits the inflammatory agents that accompany traumatic brain injury. Brain Res. 2005;1049:112–119.
84. Janes AC, Pizzagalli DA, Richardt S, Frederick BD, Chuzi S, Pachas G, et al. Brain reactivity to smoking cues prior to smoking cessation predicts ability to maintain tobacco abstinence. Biol Psychiatry. 2010;67:722–729.
85. Thoma R, Mullins P, Ruhl D, Monnig M, Yeo RA, Caprihan A, et al. Perturbation of the glutamate–glutamine system in alcohol dependence and remission. Neuropsychopharmacology. 2011;36:1359–65.
86. Wiers CE, Cunningham SI. Tomasi DG, Ernst T, Chang L, Shokri-Kojori E et al. Elevated thalamic glutamate levels and reduced water diffusivity in alcohol use disorder: association with impulsivity. Psychiatry Res: Neuroimaging. 2020; 305: epub ahead of print 30 November; https://doi.org/10.1016/j.pscychresns.2020.111185.
87. Liu X-L, Li L, Li J-N, Tang J-H, Rong J-H, Liu B, et al. Quantifying absolute glutamate concentrations in nucleus accumbens of prescription opioid addicts by using 1H MRS. Brain Behav. 2017;7:e00769.
88. Colizzi M, Weltens N, McGuire P, Lythgoe D, Williams S, Van Oudenhove L, et al. Delta-9-tetrahydrocannabinol increases striatal glutamate levels in healthy individuals: implications for psychosis. Mol Psychiatry. 2020;25:3231–40.
89. Kanaan AS, Gerasch S, García-García I, Lampe L, Pampel A, Anwander A, et al. Pathological glutamatergic neurotransmission in Gilles de la Tourette syndrome. Brain. 2017;140:218–34.
90. Rowland LM, Kontson K, West J, Edden RA, Zhu H, Wijtenburg SA, et al. In vivo measurements of glutamate, GABA, and NAAG in schizophrenia. Schizophr Bull. 2013;39:1096–104.
91. Korenic SA, Klingaman EA, Wickwire EM, Gaston FE, Chen H, Wijtenburg SA, et al. Sleep quality is related to brain glutamate and symptom severity in schizophrenia. J Psychiatr Res. 2020;120:14–20.
92. Gao M, Aveyard P, Lindson N, Hartmann-Boyce J, Watkinson P, Young D, et al. Association between smoking, e-cigarette use and severe COVID-19: a cohort study. Int J Epidemiol. 2022;51:1062–72.
93. Rubin DT, Ananthakrishnan AN, Siegel CA, Sauer BG, Long MD. ACG clinical guideline: ulcerative colitis in adults. Am J Gastroenterol. 2019;114:384–413.

AUTHOR CONTRIBUTIONS

JON, MPD, JRA, J-BP, DG, ACD, RFT, NP, and EDL collaboratively designed the study. JON, MPD, DG, SM, and AK contributed to data acquisition. JON, MPD, JRA, J-BP, DG, RFT, and AK contributed to data analysis. JON, MPD, JRA, J-BP, DG, and EDL interpreted the data. All authors contributed to drafting or to critically revising the work for important intellectual content and gave final approval of the work. All authors agree to be accountable for all aspects of the work in ensuring that questions related to the accuracy or integrity of any part of the work are appropriately investigated and resolved.

FUNDING INFORMATION

This research was supported by award F32DA049500 to MPD, R03DA052719 to JRA and EDL, and by awards R37DA044467 and R37DA044467S to EDL and RFT acknowledges the support of a Canada Research Chair.

COMPETING INTERESTS

The authors declare no competing interests.

ADDITIONAL INFORMATION

Supplementary information The online version contains supplementary material available at https://doi.org/10.1038/s41380-023-02247-0.

Correspondence and requests for materials should be addressed to Edythe D. London.

Reprints and permission information is available at http://www.nature.com/reprints

Publisher's note Springer Nature remains neutral with regard to jurisdictional claims in published maps and institutional affiliations.